On Vertically Propagating Coastal Kelvin Waves at Low Latitudes

R. D. ROMEA[1] AND J. S. ALLEN

School of Oceanography, Oregon State University, Corvallis, OR 97331

(Manuscript received 16 August 1982, in final form 1 March 1983)

ABSTRACT

Vertically propagating coastal internal Kelvin waves (IKWs) forced by the alongshore component of the wind at the coast are studied, utilizing an f-plane model of a continuously stratified ocean with a vertical eastern boundary. With an infinitely deep ocean, several initial value problems that illustrate the basic properties of the forced flow are presented. For a wind stress at the surface that is localized in time and space, changes in amplitude and frequency with depth are predicted. Far from the forcing region, the response represents a non-uniform wavetrain of free IKWs characterized by local frequencies and wavenumbers. The group velocity vector is directed downward and poleward while the phase propagation is upward and poleward. For forcing by a traveling wind with fixed frequency σ and horizontal wavenumber l and with step functions at an alongshore location $y = 0$ and at $t = 0$, the response near and far from $y = 0$ has a different qualitative behavior. Near $y = 0$ a maximum in alongshore velocity v propagates downward until it intersects the ray path that passes through $y = 0$ at the surface for a free IKW with frequency σ. Subsequently the maximum remains on the ray path. Far from $y = 0$, a traveling wave wind stress forces a component that decays with depth from the surface and that is trapped within a Rossby radius of the coast. For a poleward traveling wind, an additional component is forced, which represents a coastally trapped IKW with negative vertical group velocity and upward phase propagation. The two limits $|ly| \ll 1$ and $|ly| \gg 1$ approximately model forcing near and far from the equator. The model with an infinitely deep ocean applies for initial value problems before disturbances generated at the surface reach the bottom. For longer time, the model applies for frequencies and wavenumbers where motions are damped by internal dissipation before they reach the bottom. A solution obtained with a bottom at $z = -H$ shows that, for forcing with a step function at $y = 0$, the results obtained with an infinitely deep ocean apply for $|z| \ll H$ and $|ly| \ll 1$.

1. Introduction

Vertically propagating internal waves in the ocean are generally constrained such that $f < \omega < N$, where ω is the radian frequency, f the Coriolis parameter, and N is the Brunt–Väisälä frequency. For $\omega < f$, vertical propagation is possible when one of the horizontal wavenumbers is imaginary, a condition that is satisfied for equatorially trapped waves with meridional modal structure or for coastally trapped waves that propagate along a boundary and that decay exponentially with distance from the coast (internal Kelvin waves). Such low-frequency vertically propagating waves have been observed near the equator, e.g., by Weisberg *et al.* (1978) who find that equatorially trapped motions in the Gulf of Guinea are downward propagating, not vertically standing modes. Also, from observations on the continental slope in the Gulf of Guinea, Picaut (1981) reports an upward phase propagation of temperature associated with the seasonal upwelling cycle, which he interprets as the signature of a coastal Kelvin wave that propagates westward and vertically.

Recent observations on the Peru continental shelf and slope during ESACAN (Estudio del Sistema de Afloramiento Costero en el Area Norte), the joint German–Peruvian experiment at 5°S latitude, and during the CUEA (Coastal Upwelling Ecosystems Analysis) JOINT-2 experiment at 15°S latitude indicate that vertically propagating waves exist over the slope at low frequencies (period $T = 2\pi/\omega > 20$ days). For example, Fig. 1 shows low-pass filtered alongshore wind at Talara (4°34′S) and alongshore current velocity and temperature from the ESACAN C2 mooring which is on the continental slope in 1360 m of water. The current velocity data show a low frequency pulse-like event that amplifies between 86 m and 560 m depth, and that appears to propagate vertically downward between 86 and 560 m. The relationship between velocity and temperature at 560 and 860 m suggests that at those depths there is a phase propagation upward of both signals with velocity and temperature $\pi/2$ out-of-phase.

In this study we analyze the dynamics of the second class of subinertial vertically propagating waves described above, namely coastally-trapped internal Kelvin waves (hereafter referred to as IKWs). We focus on low latitude dynamics, where the Rossby radius scale, which is the natural offshore length scale for

[1] Present affiliation: Department of Oceanography, Florida State University, Tallahassee, FL 32306

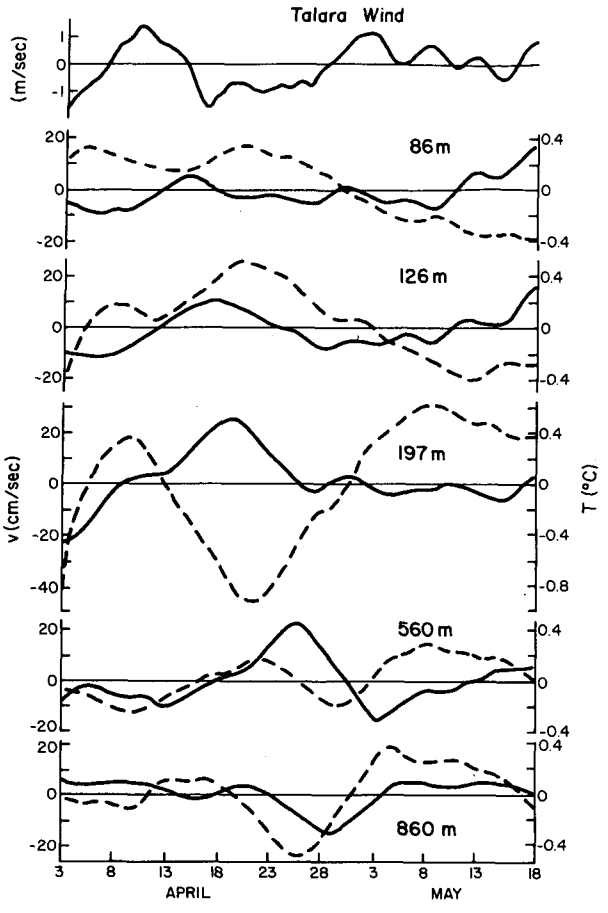

FIG. 1. Time series of low-pass filtered alongshore wind from Talara (4°34'S) (top plot) and of northward current v (solid line) and temperature T (dashed line) from the ESACAN C2 mooring, which was on the continental slope in 1360 m of water at 5°S latitude. The low-pass filter has a half power point of 8.5 days.

baroclinic motions, is much larger than the shelf-slope width. For this case, the shelf-slope region appears like a vertical wall, and we adopt a model with a vertical coastal boundary. We pay attention to the low frequency behavior ($T \approx 20$–40 days) but specify that the waves are still coastally trapped (see Appendix A).

Typically, oceanic problems are solved with the bottom boundary condition $w = 0$. Recently it has been suggested that the ocean might be better modeled in some frequency–wavenumber regimes by neglecting the effects of a bottom boundary and assuming that the ocean is infinitely deep (Wunsch, 1977; Philander, 1978). We utilize a model of this type in Sections 2 and 3, where we consider the response of a rotating stratified f-plane ocean with a rigid lid, forced by an alongshore wind stress at the coast. The forced response for several different types of wind stress is calculated and shows components that are trapped near the surface and components that propagate vertically.

The assumption of infinite depth is justified if the bottom is highly dissipative, and scatters energy rather than reflecting it uniformly, or if internal motions generated at the surface dissipate before the energy can reflect off the bottom and travel back toward the surface (Wunsch, 1978). In order to assess the frequency–wavenumber regimes where frictional processes justify the neglect of a bottom boundary, the effect of internal dissipation is included in Section 4 and the dissipation time scale is compared to the time required for initial disturbances to propagate vertically from the surface to the bottom. The forced response with a bottom boundary is calculated in Section 5 and compared to the results of Sections 2 and 3 in order to assess further the space and time scales where the analyses of Sections 2 and 3 are valid. To generalize the f-plane results, the Coriolis parameter is regarded in Appendix A as a slowly varying function on the alongshore scale of the waves. Finally the oceanic implications of the results are discussed in Section 6.

2. Theoretical formulation

We consider a continuously stratified ocean with an eastern boundary that rotates on an f-plane in the Northern hemisphere. Cartesian coordinates (x, y, z) are utilized with x positive *westward*, y positive *southward*, and z positive vertically upward. There is a rigid lid on top ($z = 0$), a straight north–south coastline at $x = 0$, and the fluid is unbounded for $x \to \infty$, $z \to -\infty$. The problem is linearized by the assumption that the motion results in negligible nonlinear fluid accelerations and in small departures from an equilibrium stable density distribution $\bar{\rho}(z)$. The hydrostatic approximation is utilized and we consider interior motions away from frictional boundary layers. The long wave assumptions for coastal trapped waves are made, i.e., we assume that $\omega \ll f$ and that the characteristic alongshore scale L is large relative to the internal Rossby radius of deformation.

With the above assumptions, the governing equations are

$$-fv = -p_x/\rho_0, \tag{2.1a}$$

$$v_t + fu = -p_y/\rho_0, \tag{2.1b}$$

$$0 = -p_z - g\rho, \tag{2.1c}$$

$$u_x + v_y + w_z = 0, \tag{2.1d}$$

$$\rho_t + w\bar{\rho}_z = 0, \tag{2.1e}$$

where subscripts denote partial differentiation. The variables (u, v, w) are the velocity components in the (x, y, z) directions, t is time, p pressure, and g the acceleration of gravity. The total density is given by

$$\rho_T(x, y, z, t) = \rho(x, y, z, t) + \bar{\rho}(z) + \rho_0, \tag{2.2}$$

where ρ_0 is a constant.

Eqs. (2.1a–e) may be combined into a single equation for the pressure:

$$[p_{xx} + f^2(p_z/N^2)_z]_t = 0, \quad (2.3)$$

where

$$\rho_0 f^2 u = -p_{xt} - f p_y, \quad (2.4)$$

$$\rho_0 w = -N^{-2} p_{zt}, \quad (2.5)$$

and where $N^2 = -g\bar{\rho}_z/\rho_0$ is the square of the Brunt–Väisälä frequency.

We assume, consistent with the long wave approximation, that only the alongshore component of wind stress is important and that it is approximately constant over the scale of the Rossby radius. The alongshore wind stress acts as a driving mechanism through suction of fluid into the surface Ekman layer at the coast. An offshore or onshore mass flux in the upper Ekman layer produces the equivalent of a sink or source-like flow below the Ekman layer at the coast. The vertical extent of the region is sufficiently small so that the corner acts very nearly as a point sink or source for the flow below the Ekman layer (e.g., Pedlosky, 1969; Allen, 1973; Pedlosky, 1974). Consequently, we specify a forced boundary condition at the surface which represents an Ekman suction in the upper coastal corner at $x = 0$, $z = 0$ and no flow through the vertical boundary at $z = 0$, i.e.,

$$p_{xt} + f p_y = f\tau(y, t)\delta(z), \quad \text{at} \quad x = 0, \quad (2.6)$$

where $\delta(z) = 0$, $z \neq 0$, and

$$\int_{-H}^{0} \delta(z)dz = 1. \quad (2.7)$$

The remaining boundary conditions are

$$p_{zt} = 0, \quad \text{at} \quad z = 0, \quad (2.8)$$

$$p_x, p_y, p_z < \infty, \quad \text{as} \quad x \to \infty, \quad z \to -\infty. \quad (2.9a, b)$$

Condition (2.8) specifies no normal flow through the top, while (2.9a, b) follow from (2.1a), (2.4), (2.5) and the requirement that the energy be finite as $x \to \infty$ or $z \to -\infty$.

We consider initial value problems where

$$\tau = 0, \quad p = 0, \quad \text{for} \quad t < 0. \quad (2.10)$$

a. Free waves

Before solving the forced problem, it is useful to obtain the free wave solution to (2.3) for a vertically unbounded fluid governed by a homogeneous version of (2.6) and without condition (2.8).

We assume N^2 is a constant and seek a free wave solution of the form

$$p(x, y, z, t) = \phi(x)\,\mathrm{Re}\{\exp[-i(\omega t - ly - mz)]\}, \quad (2.11)$$

where l and m are wavenumbers, and Re denotes the real part. Substituting (2.11) in (2.3), (2.6) (with $\tau = 0$), and (2.9a), we obtain

$$\phi_{xx} - (fm/N)^2\phi = 0, \quad (2.12)$$

$$\phi_x - (fl/\omega)\phi = 0, \quad \text{at} \quad x = 0, \quad (2.13a)$$

$$\phi, \phi_x < \infty, \quad \text{as} \quad x \to \infty. \quad (2.13b)$$

The solution to (2.12) subject to (2.13a, b) is

$$\phi = \exp(flx/\omega), \quad (2.14)$$

where the dispersion relation is

$$\omega = -Nl|m|. \quad (2.15)$$

The condition (2.13b) imposes the familiar restriction,

$$l/\omega < 0, \quad (2.16)$$

i.e., free coastally trapped subinertial waves propagate with the boundary on their right side (poleward toward $-y$ with our model). The dispersion relation (2.15) gives a phase velocity with vertical component ω/m and a group velocity with vertical component $\partial\omega/\partial m = -\omega/m$. The group and phase velocities are oppositely directed, e.g., for $\omega/m > 0$, the vertical component of the phase velocity is directed upward while the vertical group velocity is downward.

b. Solution to the forced problem

The solution to (2.3) subject to (2.6)–(2.10) and the radiation condition may be conveniently represented in terms of its Fourier cosine transform in z:

$$\hat{p}(x, y, m, t) = \int_0^\infty p(x, y, z, t)\cos mz\,dz, \quad (2.17a)$$

$$p(x, y, z, t) = (2/\pi)\int_0^\infty \hat{p}(x, y, m, t)\cos mz\,dm. \quad (2.17b)$$

Multiplying (2.3), (2.6) and (2.9a) by $\cos(mz)$ and integrating over z from 0 to ∞, we obtain

$$\hat{p}_{xx} - (mf/N)^2\hat{p} = 0, \quad (2.18a)$$

$$\hat{p}_{xt} + f\hat{p}_y = f\tau(y, t), \quad \text{at} \quad x = 0, \quad (2.18b)$$

$$\hat{p}_y, \hat{p}_x < \infty, \quad \text{as} \quad x \to \infty. \quad (2.18c)$$

Eqs. (2.18a–c) have a solution

$$\hat{p} = \hat{Y}(y, m, t)\exp(-fmx/N), \quad (2.19)$$

where

$$-(m/N)\hat{Y}_t + \hat{Y}_y = \tau(y, t). \quad (2.20)$$

Eq. (2.20) is a forced first-order wave equation for the (y, t) structure of the response and may be easily solved for various $\tau(y, t)$. In particular, we may obtain a formal solution for general $\tau = \hat{F}(y)\hat{T}(t)$ by first

considering the solution to (2.20) for a wind stress of the form

$$\tau(y, t) = \tilde{F}(y)\delta(t), \tag{2.21}$$

where $\delta(t)$ is the Dirac-delta function and where the initial condition corresponding to (2.10) is

$$\hat{Y}(0) = 0. \tag{2.22}$$

With (2.21) and (2.22), the solution to (2.20) is

$$\hat{Y} = -(N/m)\tilde{F}(y + Nt/m), \tag{2.23}$$

which, together with (2.17b) and (2.19), gives

$$p = p_D = -(2N/\pi)\int_0^\infty \tilde{F}(y + Nt/m) \times \exp(-fmx/N)m^{-1}\cos(mz)dm. \tag{2.24}$$

The subscript D identifies (2.24) as the response to forcing by a wind stress whose time dependence is given by a delta function. The term p_D represents a Green's function for a wind stress concentrated in time. Now if a wind stress with general time dependence $\tau(y, t) = \tilde{F}(y)\tilde{T}(t)$ is applied, the pressure is given by

$$p = \int_0^t p_D(x, y, z, t - \alpha)\tilde{T}(\alpha)d\alpha. \tag{2.25}$$

Alternately, for simple τ is may be easier to solve (2.20) for $\hat{Y}$ directly and utilize (2.19) and (2.17b) to obtain p.

3. Examples

To gain an appreciation for some of the features of the solutions, we examine three idealized situations for the y and t variation of τ.

a. Example A

We first choose a wind stress of the form

$$\tau(y, t) = \delta(y)\delta(t)\tau_A. \tag{3.1}$$

The solution, which may be obtained directly from (2.24), is

$$p = (2/\pi)(N\tau_A/y)\cos(Ntz/y)\exp(fxt/y), \quad y < 0. \tag{3.2}$$

The disturbance at $y = 0$ acts like a source that emits waves of all frequencies and wavelengths. The pressure exhibits an exponential decay in x for fixed y and decays like $|y|^{-1}$ in the alongshore direction. In Fig. 2, v obtained from (3.2) is plotted as a function of t for various values of z in terms of scaled variables defined in the figure caption. We show v rather than p because velocity may be directly compared with current observations. Frequency variations with depth are evident. The envelope $t\exp(fxt/|y|)$, which is the response at $z = 0$, governs the initial growth of v at all depths to some maximum value and its subsequent decay with time.

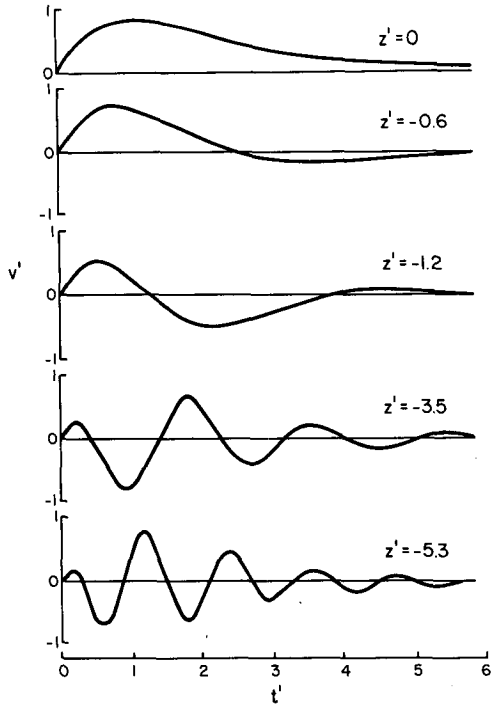

FIG. 2. Scaled alongshore velocity $v' = [(2/\pi)N\tau_A(\rho_0|y|fx)^{-1}]^{-1} \times v$ as a function of $t' = fxt/|y|$ and $z' = Nz(fx)^{-1}$ for Example A [$\tau(y, t) = \delta(y)\delta(t)\tau_A$].

For $|Ntz/y| \gg 1$, the waves behave locally like simple harmonic waves of a certain local frequency and wavelength which move in accordance with the relation

$$\theta = Ntz/y = \text{constant}, \tag{3.3}$$

where θ is the phase and both z, $y < 0$. The local frequency and wavenumbers are given by (Whitham, 1974, p. 375)

$$\omega_0 = -(\partial\theta/\partial t) = -Nz/y, \tag{3.4}$$

$$m_0 = \partial\theta/\partial z = Nt/y, \tag{3.5}$$

$$l_0 = \partial\theta/\partial y = -Ntz/y^2, \tag{3.6}$$

when variations in wavenumber l_0 are small over a wavenumber interval, i.e., $l_0^{-1}\Delta l \ll 1$, which implies $|Ntz/y| \gg 1$. Thus the frequency varies as a function of position while the wavenumbers change with both position and time. For fixed time, waves farther in y from the source have longer wavelengths.

The alongshore and vertical components of the local phase velocity may also be computed. These are

$$c_{p0}^{(z)} = -(\partial\theta/\partial t)/(\partial\theta/\partial z) = \omega_0/m_0 = -z/t, \tag{3.7a}$$

$$c_{p0}^{(y)} = -(\partial\theta/\partial t)/(\partial\theta/\partial y) = \omega_0/l_0 = y/t, \tag{3.7b}$$

and the phase velocity is directed upward and poleward. For fixed y or z, the phase moves more slowly as time increases, but for fixed t more rapidly as $|y|$ or $|z|$ increase.

We may express the local frequency in terms of the local wavenumbers, which gives

$$\omega_0 = Nl_0/m_0. \tag{3.8}$$

Local group velocity components are

$$c_{g0}^{(z)} = \partial\omega_0/\partial m_0 = -Nl_0/m_0^2 = z/t, \tag{3.9}$$

$$c_{g0}^{(y)} = \partial\omega_0/\partial l_0 = N/m_0 = y/t. \tag{3.10}$$

The local group velocity vector associated with waves of fixed wavenumbers l_0 and m_0 at time t is directed downward and poleward. Comparison of (3.8), (3.9), and (3.10) with the corresponding expressions obtained from (2.15) for the free wave example in Section 2 shows, as expected, that for $|Ntz/y| \gg 1$, the response behaves like a nonuniform wavetrain of free waves with local frequencies and wavenumbers. With $y/t = N/m_0$ from (3.5), the condition $|Ntz/y| \gg 1$ also corresponds to $|m_0 z| \gg 1$, which specifies that the disturbance must be much more than a local wavelength away from the surface.

b. Example B

We next consider

$$\tau(y, t) = \delta(y)H(t)T(t)\tau_B, \tag{3.11}$$

where $H(t)$ is the Heaviside function $H(t) = 0$, $t < 0$; $H(t) = 1$, $t > 0$. This example represents forcing by a wind stress that is localized in space and that has a general time behavior initiated at $t = 0$. Substitution of (3.11) in (2.25) gives

$$p = -(2/\pi)(\tau_B N/|y|)\exp(-fxt/|y|) \times \int_0^t \cos[Nz(t-\alpha)/|y|]\exp(fx\alpha/|y|)T(\alpha)d\alpha. \tag{3.12}$$

The special case $T(t) = \delta(t)$ corresponds to Example A and yields the same answer.

If we assume

$$T(t) = \mathrm{Re}[\exp(-i\sigma t)], \tag{3.13a}$$

and scale the variables as

$$x' = x(\sigma'|y|)^{-1}, \quad z' = (N/\sigma)(z/|y|), \quad t' = \sigma t, \quad \sigma' = \sigma/f, \quad p' = p/[(2/\pi)(N/\sigma)\tau_B], \quad v' = v[(2/\pi)(N/\sigma)\tau_B(\rho_0\sigma|y|)^{-1}]^{-1}, \tag{3.13b}$$

the evaluation of (3.12) gives, with (3.13a),

$$p' = \mathrm{Re}\{y^{-1}(B^2 + z'^2)^{-1}[B\exp(-it') - (B\cos(t'z') - z'\sin(t'z'))\exp(-x't')]\}, \quad y < 0, \tag{3.14a}$$

where

$$B = x' - i. \tag{3.14b}$$

The first term in the brackets represents a response at the forcing frequency σ. The remaining two terms are transients which, for fixed y and $x > 0$, decay exponentially with t and are coastally trapped.

The initial response for $t' \leq 12$ where the transients are still important is illustrated in Fig. 3. The phase propagation is upward, consistent with a downward propagation of energy from the surface, while a maximum in v propagates from the surface downward. Examination of (3.14) for $x't' \gg 1$, when the transient terms have decayed, shows a subsurface maximum of v at $z' = -1$. From (2.15), this is the ray path $dz/dy = (\partial\omega/\partial m)/(\partial\omega/\partial l)$ that passes through $y = 0$, $z = 0$ for a freely propagating IKW of frequency $\omega = \sigma$. Fig. 3 shows the maximum in v propagating downward from the surface to $z' = -1$, where it intersects the IKW free wave ray path. Subsequently, the maximum in v remains at $z' = -1$.

c. Example C

Finally, we examine a more general wind stress,

$$\tau(y, t) = H(t)H(-y)F(y)T(t)\tau_C, \tag{3.15}$$

where the wind has a general y structure for $y < 0$.

The substitution of (3.15) in (2.24) and (2.25) gives

$$p = -(2/\pi)N\tau_C \int_0^t T(\alpha)d\alpha \times \int_0^{|y|} F(\beta - |y|)\exp[-fx(t-\alpha)/\beta] \times \cos[N(t-\alpha)z/\beta]\beta^{-1}d\beta, \quad y < 0. \tag{3.16}$$

A special case of interest is

$$F(y)T(t) = \mathrm{Re}\{\exp[-i(\sigma t - ly)]\}. \tag{3.17}$$

The substitution of (3.17) in (3.16) and the subsequent evaluation of the integral over α yields p.

An alternate representation for p may be obtained by substituting (3.15) and (3.17) in (2.20) and solving (2.20) directly for $\hat{Y}$ by the method of characteristics.

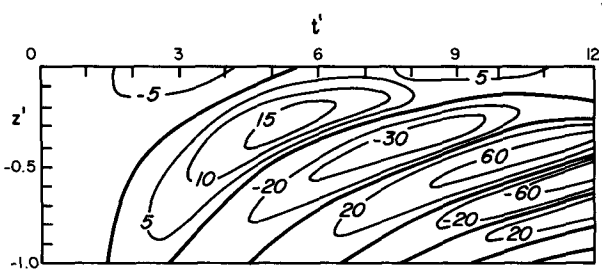

FIG. 3. Scaled alongshore velocity $v' = [(2/\pi)N\tau_B(\rho_0\sigma^2|y|)^{-1}]^{-1} \times v$ as a function of $t' = \sigma t$ and $z' = (N/\sigma)(z/|y|)$ with $x' = x/(\sigma'|y|) = 0.04$, for Example B [$\tau(y, t) = \delta(y)H(t)\tau_B \exp(-i\sigma t)$].

This solution is

$$\hat{Y} = K_1 \exp(-i\sigma t)[\exp(ily) - \exp(-i\sigma my/N)], \quad Nt/m \geq -y, \tag{3.18a}$$

$$\hat{Y} = K_1 \exp(ily)[\exp(-i\sigma t) - \exp(iNlt/m)], \quad Nt/m \leq -y, \tag{3.18b}$$

where

$$K_1 = -i\tau_C(m\sigma/N + l)^{-1}. \tag{3.18c}$$

With (2.19) and (2.17b), p is given by

$$p = \mathrm{Re}\left\{\int_0^\infty K_2 \exp(-i\sigma t + ily)dm - \int_0^{Nt/|y|} K_2 \exp(-im\sigma y/N - i\sigma t)dm - \int_{Nt/|y|}^\infty K_2 \exp(iNlt/m + ily)dm\right\}, \tag{3.19a}$$

where

$$K_2 = (2/\pi)K_1 \exp(-fmx/N)\cos(mz). \tag{3.19b}$$

The second integral in (3.19a) represents the effect of the step function at $y = 0$ and vanishes for $Nt/|y| \to 0$ while the third integral represents the effect of the step function at $t = 0$ (i.e., the wavefront) and vanishes for $Nt/|y| \to \infty$.

We first examine (3.19) for small y, i.e., $|ly| \ll 1$, or equivalently $|y| \ll \lambda_y/(2\pi)$, where $\lambda_y = |2\pi/l|$ is the alongshore wavelength of the wind. Evaluation of (3.19) with $|ly| \ll 1$ gives

$$v' = -\mathrm{Re}\langle(x'^2 + z'^2)^{-1}(B^2 + z'^2)^{-1}\{\exp(-it')E + \exp(-x't')[-E\cos(z't') - z'(B + x')\sin(z't')]\}\rangle, \quad y < 0, \tag{3.20a}$$

where

$$E = -Bx' + z'^2, \tag{3.20b}$$

and where B is given by (3.14b). This result is also obtained with (3.16), (3.17), and $|ly| \ll 1$.

Fig. 4 shows v' from (3.20) as a function of z' and t'. A subsurface maximum of v' travels downward to $z' = -1$ where it remains. In Example B this behavior was found for $F(y) = \delta(y)$, while here a similar behavior is observed which is evidently associated with the step function at $y = 0$.

For large time ($x't' \gg 1$) when the transient terms have decayed, (3.20) is asymptotically equal to

$$v' \sim \tfrac{1}{2}[\sin(t')x'(2/I - I_-^{-1} - I_+^{-1}) + \cos(t')(\mu_+/I_+ - \mu_-/I_-)], \quad y < 0, \tag{3.21}$$

where

$$I = x'^2 + z'^2, \tag{3.22a}$$

$$I_\pm = x'^2 + \mu_\pm^2, \tag{3.22b}$$

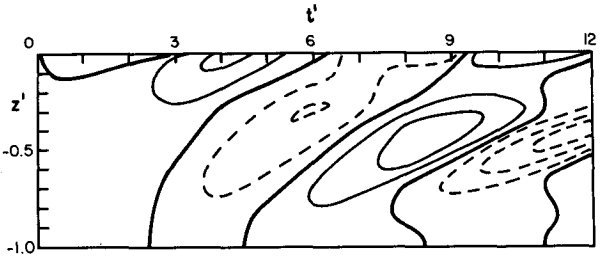

FIG. 4. Scaled alongshore velocity $v' = [(2/\pi)N\tau_C(\rho_0\sigma^2|y|)^{-1}]^{-1} \times v$ as a function of $t' = \sigma t$ and $z' = (N/\sigma)(z/|y|)$ with $x' = x/(\sigma'|y|) = 0.04$, from Example C [$\tau(y, t) = H(-y)H(t)\tau_C \exp\{-i(\sigma t - ly)\}$] for the limiting case $|ly| \ll 1$. Dark lines: contours of $v' = 0$; light lines: $v' > 0$; dashed lines $v' < 0$; contour interval: 1.

$$\mu_\pm = z' \pm 1. \tag{3.22c}$$

Note that (3.21) corresponds to the solution that may be obtained directly by solving (2.20) and (2.22) with $\tau(y, t) = H(-y)\exp(-i\sigma t)$ and with a radiation condition that restricts the solution to have energy propagating away from the source at $x = 0$, $z = 0$. For $x' \ll 1$, a maximum in v' occurs at the surface and near the line $\mu_+ = 0$, that is the ray path passing through $y = 0$, $z = 0$ for a free IKW of frequency σ. The maximum at the surface is associated with the forcing at the surface while the maximum near $\mu_+ = 0$ is associated with the step function at $y = 0$. This behavior is illustrated in Figs. 5a–d, which show the magnitude and phase of V, where $v' = V\exp(-it')$ (from (3.20) with $x't' \gg 1$) as a function of y and z' and as a function of x' and z'. The subsurface maximum along the free IKW ray path is evident in Fig. 5a. Fig. 5c shows that the subsurface maximum is strongest near the coast and weakens with increasing x'. The maximum of v' near the surface is also evident on Figs. 5a, c. The phase plots shown on Figs. 5b, d indicate that there is a 180° phase difference from the surface to below the subsurface maximum, with an upward phase propagation. The phase plot shown in Fig. 5d indicates relatively small offshore phase differences for $|z'| < 1$ and shows nearshore motions leading for $|z'| > 1$.

For large $|y|$ and large t, i.e., for $|ly| \gg 1$ and $fxt/|y| \gg 1$, the last two integrals in (3.19a) vanish and only the first integral remains. This limit gives p far from the region influenced by the step function in y and after transient components have decayed. The remaining first integral in (3.19a) corresponds to the solution that may be obtained directly by solving (2.20) with $\tau(y, t) = \exp[-i(\sigma t - ly)]$.

In Appendix B we derive a solution (B20) for forcing by a traveling plane wave wind stress with a generalized integral transform in x, in a manner similar to that utilized by Huppert and Stern (1974). Using standard analysis in the complex plane, and invoking Cauchy's integral theorem, (3.19a, b), with $|ly| \gg 1$

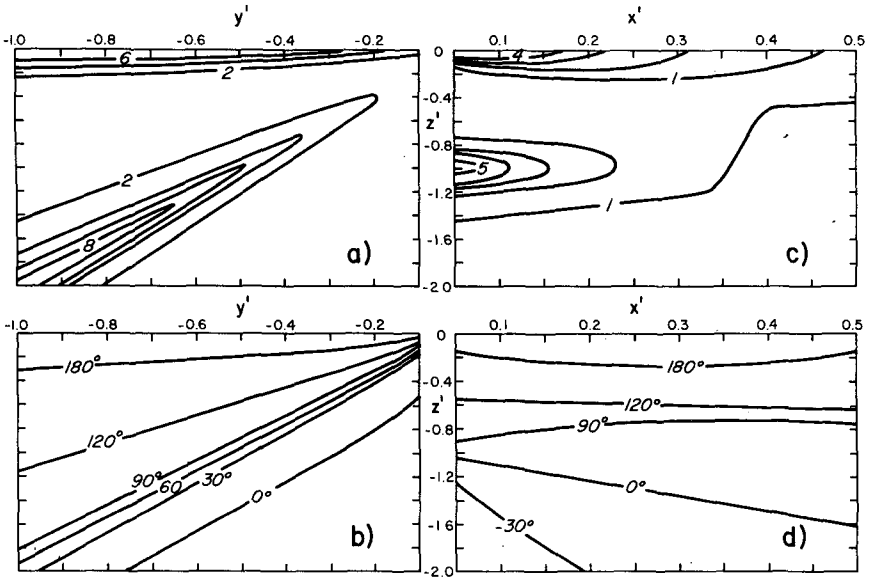

FIG. 5. Magnitude (a, c) and phase θ(b, d) of V for Example C as a function of $y' = y/y_0$ and z'(a, b) (with $x' = 0.04$) and as a function of x' and z'(c, d) (with $y' = 1$) where $v' = V \times \exp(-it')$. Limiting case $|ly| \ll 1$, $x't' \gg 1$. The scale y_0 is the alongshore location where the subsurface maximum intersects $z' = -1$. Scaling the same as in Fig. 4. $\theta_1 > \theta_2$ implies 2 leads 1.

and $|fxt/y| \gg 1$ may be shown to be asymptotically equal to (B20).

Evaluation of the first integral in (3.19a), or, alternately, the integral in (B20), yields

$$p \sim \mathrm{Re}\langle(\pi\sigma)^{-1}N\tau_C \exp[-i(\sigma t - ly)] \exp(flx/\sigma) \times \{i[\exp(iNlz/\sigma)Ei(-flx/\sigma - iNlz/\sigma) + \exp(-iNlz/\sigma)Ei(-flx/\sigma + iNlz/\sigma)] - 2(\sigma/|\sigma|)H(-l/\sigma)\pi \exp(-iNlz/|\sigma|)\}\rangle, \quad y < 0, \quad (3.23)$$

where Ei is the exponential integral function (Gradshteyn and Ryshik, 1980, p. 925) and where $H(-l/\sigma) = 1$ for $l/\sigma < 0$ and 0 for $l/\sigma > 0$.

The response is composed of two parts, one of which (the last term in braces) is forced only for $l/\sigma < 0$ and represents a coastal IKW with vertical wavenumber $m = -Nl/|\sigma|$ and negative vertical group velocity $c_g^{(z)} = -\sigma/m$. The offshore trapping scale (Rossby radius scale) is $-\sigma/fl$. The remaining two terms in (3.23) represent a forced response which decays as $|z|^{-2}$ for $|z|$ large and which exhibits the proper behavior at $x = 0$, $z = 0$ to satisfy (2.6).

The magnitude of the alongshore velocity associated with the surface trapped response (calculated numerically from the integral in (B21)) is plotted for several depths as a function of $f|l/\sigma|x$ in Fig. 6 for both poleward ($l/\sigma < 0$) and equatorward ($l/\sigma > 0$) traveling wind. For $l/\sigma < 0$, the magnitude of the downward propagating IKW is also plotted for comparison, and the propagating component may be seen to be the dominant contribution to the forced response for $N|l/\sigma|z < -0.5$. The offshore structure of the surface trapped response is depth dependent and also differs for $l/\sigma \gtrless 0$. In both cases, near the surface the magnitude of the response grows as a function of x to some maximum near $f|l/\sigma|x = 0.2$ and decays with a Rossby radius scale for $f|l/\sigma|x > 0.2$.

Fig. 7 shows v at $x = 0$ for various z as a function of $\theta = \sigma t - ly$ with $l/\sigma < 0$. The outstanding feature is the reversal of phase with depth, where the signal at $N|l/\sigma|z = -0.2$ lags the signal above and leads the signal below. The phase behavior near the surface reflects the superposition in time of the vertically propagating and the surface trapped components, while for $N|l/\sigma|z < -0.5$, the vertically propagating component dominates the response and the phase lag is consistent with a downward propagating IKW (the dashed line in Fig. 7 represents the phase lag expected for a free downward propagating IKW).

4. Internal dissipation

The theory presented in Sections 2 and 3 is limited by the neglect of bottom topography. For forcing at the surface, an initial disturbance must propagate from the surface to the bottom and back to a subsurface point z before the effect of the bottom is felt at z. The time $T_t = H_0/c_g^{(z)}$ it takes for an internal Kelvin wave with frequency ω and horizontal wavenumber l to propagate at its group velocity from the surface to the bottom $z = -H_0$, as a function of $\omega' = \omega/f$ and $l' = Ll$ is, in dimensionless form, $t^* = f^2LT_t/(NH_0) = l'/\omega'^2$, where L is a characteristic

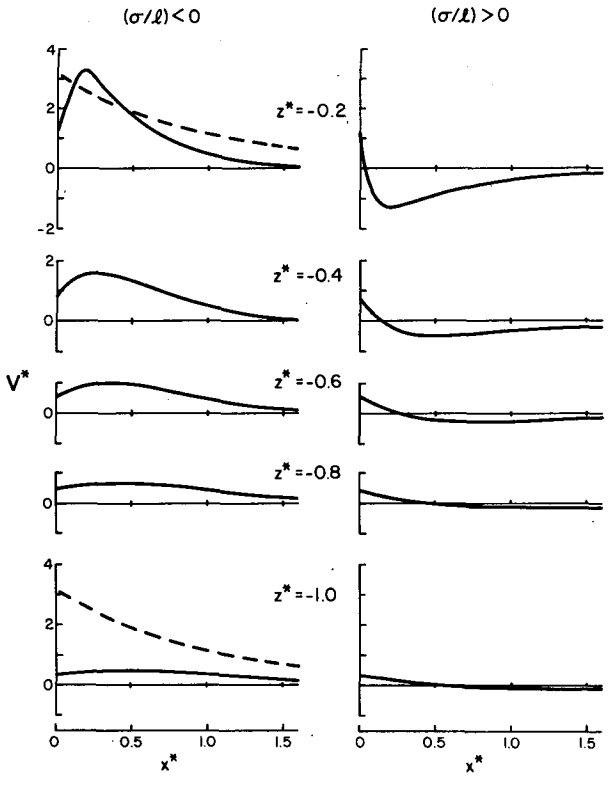

FIG. 6. Scaled alongshore velocity $V^* = V/[(2/\pi)N\tau_C l(\rho_0\sigma^2)^{-1}]$ for Example C, obtained for the limiting case $fxt/|y| \gg 1$ and $|ly| \gg 1$, as a function of $x^* = flx/\sigma$ for various $z^* = Nz|l/\sigma|$, where $v = V\exp[-i(\sigma t - ly)]$. The response is plotted for $l/\sigma > 0$ and $l/\sigma < 0$. The scale for V^* at $z^* = -0.2$ applies to V^* at all depths. The solid line represents the vertically trapped response while the dotted line represents the magnitude of the vertically propagating IKW. The two components are $\pi/2$ out of phase in time and are plotted on the same figure in order to compare magnitudes. The offshore distance $x^* = 1$ corresponds to the Rossby radius scale.

alongshore length scale. Waves with lower frequency or larger wavenumber l travel more slowly. As an example, with $H_0 = 2$ km, and with a stratification approximated by $N = 4 \times 10^{-3}$ s^{-1}, a wave with $\lambda_y = 1000$ km, $T = 2\pi/\sigma = 5.7$ days takes approximately 3.5 days to reach the bottom while a wave with $T = 25$ days takes about 69 days.

Internal dissipation, which causes an energy decay with time, may prevent the energy that is reflected at the bottom from affecting the response near the surface. For such cases, the response obtained with an infinitely deep ocean may be valid near the surface for much longer times than indicated by the above travel time calculation. We next examine this point, using a model which allows the vertical mixing of heat and momentum in the deep ocean.

The linearized equations are (2.1a), (2.1c), (2.1d) and

$$v_t + fu = -p_y\rho_0 + \nu v_{zz}, \tag{4.1a}$$

$$\rho_t + \bar{\rho}_z w = \kappa\rho_{zz}, \tag{4.1b}$$

where ν and κ are coefficients of vertical eddy viscosity and diffusivity, respectively, assumed constant.

Eqs. (2.1a, c, d) and (4.1a, b) may be combined to form a single equation for p, given by

$$[p_{xx} + (f/N)^2 p_{zz}]_t - \nu[p_{xx} + (f/N)^2\,\mathrm{Pr}^{-1}p_{zz}]_{zz} = 0, \tag{4.2}$$

where $\mathrm{Pr} = \nu/\kappa$ is the Prandtl number and where for simplicity we assume that N = constant. Regularity conditions as $x \to \infty$ and $z \to -\infty$ are given by (2.9a, b) and the remaining boundary conditions are

$$p_{xt} + fp_y - \nu p_{zzx} = f\tau(y, t)\delta(z), \quad \text{at} \quad x = 0, \tag{4.3a}$$

$$p_{zt} = \kappa p_{zzz}, \quad \text{at} \quad z = 0. \tag{4.3b}$$

Eq. (4.2) and conditions (4.3a, b) are analogous to (2.3), (2.6) and (2.8) for the inviscid case.

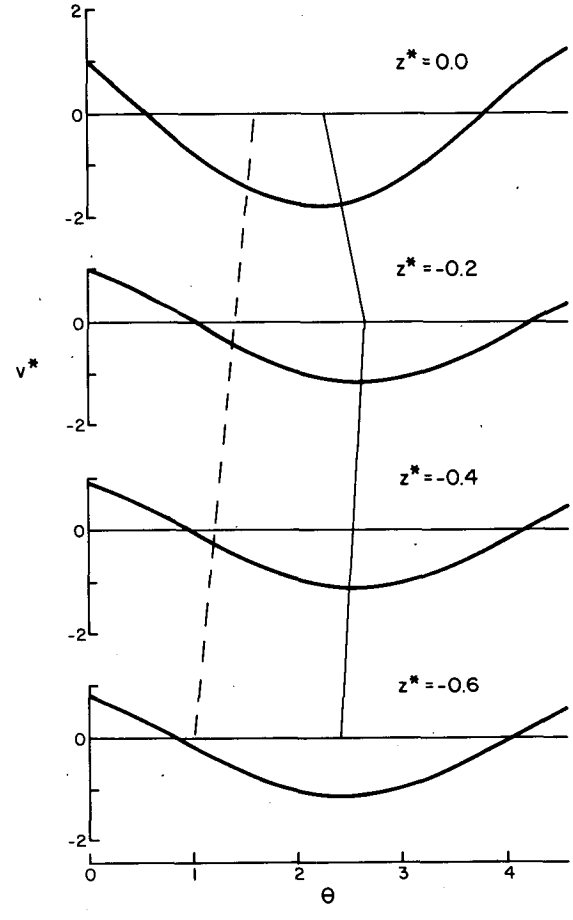

FIG. 7. Scaled alongshore velocity $v^* = v/[2N\tau_C l(\rho_0\sigma^2)^{-1}]$ at $x = 0$ for Example C obtained with the limits $fxt/|y| \gg 1$ and $|ly| \gg 1$ as a function of $\theta = \sigma t - ly$ for various $z^* = Nz|l/\sigma|$, with $l/\sigma < 0$. The straight lines connect the local maxima of v^* and indicate the vertical phase structure while the dashed line represents the vertical phase lag predicted for a free IKW with positive vertical phase velocity.

a. Free wave solution

Before solving the forced problem, we obtain the free wave solution to (4.2) for a vertically unbounded ocean subject to a homogeneous version of (4.3a) with condition (4.3b) dropped. The assumed form of the free wave is given by (2.11). The x-structure and the dispersion relation are derived in a manner similar to that in Section 2a and are given by

$$\phi = \exp[(fm/N)(1 + im^2\kappa/\omega)^{1/2} \times (1 + im^2\nu/\omega)^{-1/2}x], \quad (4.4a)$$

$$\omega = (Nl/m)(1 + im^2\kappa/\omega)^{-1/2}(1 + im^2\nu/\omega)^{-1/2}. \quad (4.4b)$$

These reduce to (2.14) and (2.15) when $\nu = \kappa = 0$. For the general case $\Pr \neq 1$, there is an offshore phase shift induced by internal dissipation, as well as a correction to the offshore structure. The frequency and hence the phase speed is modified and ω has a negative imaginary part which corresponds to a decay with time.

The special case $\Pr = 1$ yields

$$\phi = \exp(fmx/N), \quad (4.5a)$$

$$\omega = Nl/m - im^2\nu, \quad (4.5b)$$

i.e., the phase speed and offshore structure are unaffected by dissipation (see (2.14) and (2.15)), but a decay with time is still present.

We may estimate a dissipation decay time,

$$T_d = (m^2\nu)^{-1} = (\omega^2/\nu)(Nl)^{-2}, \quad (4.6a)$$

from (4.5b) for the free vertically propagating waves. The ratio,

$$(T_d/T_t)(\nu H_0 N^3 f^{-4} L^{-3}) = \omega'^4/l'^3 \quad (4.6b)$$

gives a measure of the effectiveness of dissipation in damping the wave before a reflection occurs at the bottom. The waves are damped more effectively for shorter wavelength or lower frequency. For $T_d/T_t \gg 1$, the wave reflects many times at the surface and the bottom before it decays, while for $T_d/T_t \ll 1$ dissipation damps the wave before a single reflection takes place. For the parameters given above and with $\nu \approx 10$ cm^2 s^{-1}, $T_d/T_t < 1$ for $T < 30$ days, i.e., free waves are damped considerably before they reach the bottom.

b. Forced problem

As in Section 2b, we represent the solution to (4.2) subject to (4.3a, b), (2.8) and (2.9) in terms of its Fourier cosine transform in z, given by (2.17a, b). In doing this, we assume that each side of (4.3b) is zero independently, i.e., that both $w = 0$ and the perturbation density $\rho = 0$ at the ocean surface. This requirement on ρ implies that the basic state density or temperature at the surface is fixed. A more appropriate condition would specify a relationship between heat flux and other parameters. However, we are concerned mainly with the velocity structure of the forced response and the condition on ρ invoked above has been commonly utilized (Pedlosky, 1974; Allen, 1973; McCreary, 1981).

With $\Pr = 1$, the transformed equation and boundary conditions have a solution given by (2.19) where

$$-(m/N)\hat{Y}_t + \hat{Y}_y - (\nu m^3/N)\hat{Y} = \tau(y, t). \quad (4.7)$$

Eq. (4.7) is a forced first-order wave equation similar to (2.20) for the inviscid case but it contains an additional term due to internal friction. With the wind stress τ given by (3.2a) (Example A from Section 3),

$$p = (2/\pi)(N\tau_A/y)\cos(Ntz/y) \times \exp(fxt/y - \nu N^2 t^3/y^2), \quad y < 0. \quad (4.8)$$

This response is similar to the inviscid response (3.1b) except that there is a decay in time due to the effect of dissipation. At a fixed location, the damping behaves like $\exp(-\nu t^3)$, which with (3.5) may also be expressed as $\exp(-\nu m_0^2 t)$, where m_0 is the local vertical wavenumber. Thus, locally the forced response decays on the same time scale as the free waves of Section 4a.

5. Effect of a bottom boundary

a. Inviscid case

In order to examine the effects of a bottom boundary at $z = -H_0$, the radiation and regularity conditions that apply to the unbounded ocean are replaced by the boundary condition $w = 0$ at $z = -H_0$. In terms of pressure, Eq. (2.5) implies that (2.8) holds also at $z = -H_0$. The remaining equations are (2.3), (2.6) and (2.9a), where again N is assumed constant for simplicity.

In this section it is useful to define variables $\hat{x}$ and $\hat{z}$, where we scale x with the internal Rossby radius scale and z with the depth, i.e.,

$$\hat{x} = f\pi(NH_0)^{-1}x, \quad \hat{z} = z/H_0. \quad (5.1a)$$

In addition, for later use we define

$$\hat{y} = \sigma\pi(NH_0)^{-1}|y|, \quad \hat{t} = \sigma t. \quad (5.1b)$$

The solution is conveniently represented by expanding the pressure in terms of vertical modes. This gives

$$p = \sum_{n=0}^{\infty} \phi_n(x, y, t)\cos(n\pi\hat{z}). \quad (5.2)$$

Substitution of (5.2) in (2.3) and utilization of the orthogonality of the vertical eigenfunctions gives

$$\phi_{nxx} - (fn\pi)^2(NH_0)^{-2}\phi_n = 0. \quad (5.3)$$

Solving (5.3) subject to (2.9a) yields

$$\phi_n = \exp(-n\hat{x})Y_n(y, t), \quad n = 1, 2 \cdots . \quad (5.4)$$

Substitution of (5.4) and (5.2) in (2.6) yields

$$-n\pi(NH_0)^{-1}Y_{nt} + Y_{ny} = (2/H_0)\tau(y, t). \quad (5.5)$$

The $n = 0$ term is $\phi_0 = Y_0(y, t)$ and it corresponds to the representation, within $x \leqslant O[NH_0(f\pi)^{-1}]$, of the barotropic response that varies on the larger scale $L_x \gg NH_0(f\pi)^{-1}$.

For

$$\tau(y, t) = H(-y)H(t)\,\mathrm{Re}[\exp(-i\sigma t)]\tau_C, \quad (5.6)$$

we obtain

$$v = p_x(\rho_0 f)^{-1} = \mathrm{Re}\{2i\tau_C(\rho_0 H_0\sigma)^{-1} \times [\exp(-i\hat{t}) \sum_{n=1}^{\infty} L_n - \exp(-i\hat{t}) \times \sum_{n=1}^{J} L_n \exp(in\hat{y}) - \sum_{n=J+1}^{\infty} L_n]\}, \quad y < 0, \quad (5.7a)$$

$$L_n = \exp(-n\hat{x}) \cos n\pi\hat{z}, \quad (5.7b)$$

where

$$J \leqslant [\hat{t}/\hat{y}] \quad (5.7c)$$

is the largest integer less than or equal to $\hat{t}/\hat{y}$. The three sums in (5.7a) are analogous to the three integrals in (3.19a). The first sum represents the particular solution, the second satisfies the boundary condition at $\hat{y} = 0$, and the third satisfies the initial condition at $\hat{t} = 0$.

The series in (5.7a) may be summed to yield

$$v = \mathrm{Re}\,\langle 2i\tau_C(\rho_0 H_0\sigma)^{-1}\{[1 - 2q_1 \cos\pi\hat{z} + q_1^2]^{-1} \times [\exp(-i\hat{t})(1 - q_1 \cos\pi\hat{z}) - q_1^{J+1} \cos(J + 1)\pi\hat{z} + q_1^{J+2} \cos J\pi\hat{z}] - \exp(-i\hat{t})[1 - 2q_2 \times \cos\pi\hat{z} + q_2^2]^{-1} \times [1 - q_2 \cos\pi\hat{z} - q_2^{J+1} \times \cos(J + 1)\pi\hat{z} + q_2^{J+2} \cos J\pi\hat{z}]\}\rangle, \quad (5.8a)$$

where

$$q_1 = \exp(-\hat{x}), \; q_2 = \exp(-\hat{x} + i\hat{y}). \quad (5.8b, c)$$

For

$$\pi\hat{z} \ll 1, \; \hat{x} \ll 1, \quad \hat{y} \ll 1, \quad (5.9)$$

Eq. (5.8) reduces to

$$v = \mathrm{Re}\,\langle -2\tau_C y(\rho_0 H_0\sigma)^{-1}(\hat{C}\hat{D})^{-1}\{\exp(-i\hat{t}) \times (-\hat{B}\hat{x} + \pi^2\hat{z}^2) + (i\hat{y})^{-1} \exp(-J\hat{x}) \times [\hat{D} - \hat{C} \exp(-i(\hat{t} - J\hat{y}))] \times [-\hat{x} \cos J\pi\hat{z} + \pi\hat{z} \sin J\pi\hat{z}] + \exp(-J\hat{x}) \times \exp[-i(\hat{t} - J\hat{y})] \cos J\pi\hat{z}\}\rangle, \quad (5.10a)$$

where

$$\hat{B} = \hat{x} - i\hat{y}, \; \hat{C} = \hat{x}^2 + \pi^2\hat{z}^2, \quad \hat{D} = \hat{B}^2 + \pi^2\hat{z}^2. \quad (5.10b, c, d)$$

The expression for v in (5.10) may be compared to that in (3.20) which was obtained in Section 3c for an infinitely deep ocean with (3.15), (3.17) and $|ly| \ll 1$. Eq. (5.10) is similar to (3.20) but differs from it because of the integer nature of J which results from the expansion in vertical normal modes (5.2) [If $J = \hat{t}/\hat{y}$ is assumed to be a continuous variable, (5.10) reduces to (3.20) exactly.] Therefore, the initial behavior of v from (5.8), under conditions (5.9), will be qualitatively similar to that given in (3.20) and shown in Fig. 4.

The limiting solution for v as $J \to \infty$, which corresponds to long time after transients have dispersed may be obtained from (5.7a) and is given by

$$v = \tfrac{1}{2}\tau_C(\rho_0 H_0\sigma)^{-1}\{\sin\hat{t} \sinh\hat{x}[2(\cosh\hat{x} - \cos\pi\hat{z})^{-1} - (\cosh\hat{x} - \cos\hat{\mu}_-)^{-1} - (\cosh\hat{x} - \cos\hat{\mu}_+)^{-1}] + \cos\hat{t}\,[\sin\hat{\mu}_+(\cosh\hat{x} - \cos\hat{\mu}_+)^{-1} - \sin\hat{\mu}_-(\cosh\hat{x} - \cos\hat{\mu}_-)^{-1}]\}, \quad y < 0, \quad (5.11a)$$

where

$$\hat{\mu}_\pm = \pi\hat{z} \pm \hat{y}. \quad (5.11b)$$

The long time response (5.9) is periodic in $\hat{y}$ and $\hat{t}$ with a maximum in v for $z = 0$ and near $\hat{\mu}_\pm = 2k\pi$, $k = 0, 1, 2 \ldots$. Figs. 8a, b show the magnitude and phase of V, where $v = 2i\tau_C(\rho_0 H_0\sigma)^{-1}V\exp(-i\hat{t})$, from (5.8a) with $J \gg 1$, as a function of $\hat{y}$ and $\hat{z}$. The subsurface maximum along $\hat{\mu}_+ = 0$ (Fig. 8a) is associated with the ray path for a free vertically propagating IKW with frequency $\omega = \sigma$ that passes through $\hat{y} = 0$, $\hat{z} = 0$ and travels to the bottom, while the maximum along $\hat{\mu}_- = 2\pi$ is associated with the ray path of the reflected wave that propagates from the bottom to the surface. Subsequent reflections at $\hat{z} = 0$ and $\hat{z} = -1$ occur periodically in $\hat{y}$. In regions where the ray path implies downward (upward) propagation of energy, the phase velocity is directed upward (downward). This is illustrated in Fig. 8b, which shows the phase of V.

The asymptotic limit under conditions (5.9) of the long-time solution for v in (5.11) may be shown to be exactly equal to (3.21), which was obtained for an infinitely deep ocean. Hence, for forcing given by (5.6), Eq. (5.9) establishes limits on the validity of the analysis in Sections 2 and 3. For example, with the parameters chosen in Section 4, the effect of a bottom may be neglected for $|z| \ll 0.64$ km, $x \ll 196$ km, and $|y| \ll 875$ km ($T = 25$ days).

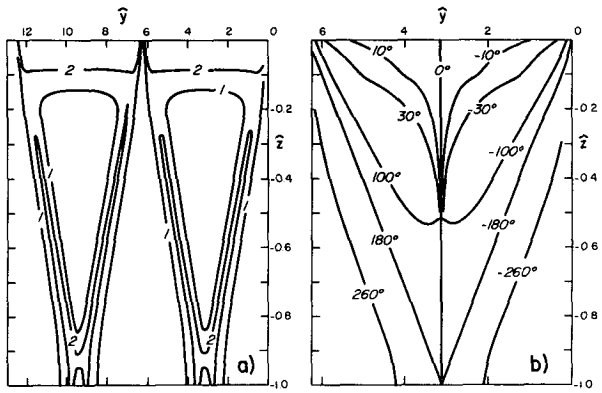

FIG. 8. Magnitude (a) and phase θ (b) of scaled alongshore velocity V as a function of $\hat{y}$ and $\hat{z}$, with $\hat{x} = 0.02$ and $\hat{t}/\hat{y} \gg 1$, where $iV \exp(-i\hat{t}) = v/[2\tau_C/(\rho_0 H_0 \sigma)^{-1}]$. Flat bottom at $\hat{z} = -1$. $\theta_1 > \theta_2$ implies 2 leads 1.

b. *Internal friction*

The inviscid analysis of the previous section predicts an infinite number of reflections at $\hat{z} = 0$ and $\hat{z} = -1$, periodic in $\hat{y}$. The effect of internal dissipation modifies this behavior. Equations and boundary conditions for this problem with friction are (4.2), (4.3a) and (4.3b), where (4.3b) also holds at $\hat{z} = -1$.

The solution for p is given by (5.2) and (5.4) where here Y_n satisfies

$$-(n\pi)(NH_0)^{-1}Y_{nt} + Y_{ny} - rn^2(n\pi)(NH_0)^{-1}Y_n = (2/H_0)\tau(y, t), \quad (5.12a)$$

$$r = \nu(\pi/H_0)^2. \quad (5.12b)$$

In the case with forcing given by (5.6),

$$v = \mathrm{Re}\{2i\tau_C(\rho_0 H\sigma)^{-1}[\exp(-i\hat{t}) \times \sum_{n=1}^{\infty} M_n - \exp(-i\hat{t}) \sum_{n=1}^{J} M_n \exp[n(i - rn^2\sigma^{-1})\hat{y}] - \sum_{n=J+1}^{\infty} M_n \exp(-rn^2\sigma^{-1}\hat{t})]\}, \quad y < 0, \quad (5.13a)$$

$$M_n = (1 + irn^2\sigma^{-1})^{-1} \exp(-n\hat{x}) \cos n\pi\hat{z}, \quad (5.13b)$$

where the three sums in (5.13a) are analogous to those in (5.7a) and where J is given by (5.7c).

The long-time behavior, which may be obtained from (5.13a) by letting $J \to \infty$ is no longer periodic in y. The effect of the step function decays rapidly with y for high mode number, and only the effect due to the lowest several modes remains. The beam pattern which results from the inviscid analysis only exists near $y = 0$.

6. Discussion

Utilizing an f-plane model with constant stratification and with a vertical boundary, we have shown that under certain conditions vertically propagating subinertial motions may be forced by the alongshore component of the wind at the coast. This simple model illustrates the essential properties of the forced flow, in particular the sensitivity of the coastal response to the exact nature of the wind forcing (i.e., the response to an initial disturbance is very different from the flow due to a steady forcing) as well as to the wind's frequency–wavenumber structure.

Based on the examples of Section 3, together with the analysis of Sections 4 and 5, we may make some general statements about the conditions for which vertically propagating coastally trapped waves might be observed in the ocean. For an initial disturbance at the surface, with a general frequency–wavenumber spectrum and large alongshore scale, downward propagating energy would be observed for those frequency–wavenumber components of the forced response that have not reflected from the bottom. Those components that have reflected from the bottom will exhibit a more complicated vertical phase dependence due to the superposition of downward and upward propagating energy. Waves with higher frequencies and longer wavelengths travel faster.

The energy of the disturbance may dissipate before a round-trip from the surface to the bottom to the surface is completed and hence internal dissipation may prevent the interference of reflected energy with downward propagating energy, even for longer time. With these conditions, one would expect to see vertically propagating waves near the surface for those frequencies and wavenumbers where they are damped effectively by internal dissipation. Internal dissipation damps the waves more effectively for shorter wavelength or lower frequency. For the parameters in Section 4, free waves are damped considerably before the wave reaches the bottom.

These simple calculations may explain why vertically standing coastally trapped waves are observed along the Peru coast in the 5–10 day band (Smith, 1978; Brink *et al.*, 1978; Romea and Smith, 1982) while relatively large phase lags are observed in the vertical for perturbations in velocity for $T > 25$ days (Fig. 1).

For cases where dissipation or long travel times may not be invoked in order to neglect the effects of reflection from the ocean bottom, an example where the wind stress is modeled by a traveling wave with a step function in y shows that the effect of a bottom may be ignored for $|z| \ll H_0/\pi$ and $|y| \ll (NH_0/\sigma\pi)$. The step function in y is an approximate model for low latitudes, where the presence of the equator introduces an effective step-function behavior to the forcing, since a wind stress applied at a location is felt only poleward of that location. With $T \approx 25$ days and with $H_0 \approx 2$ km, the effect of a bottom may be ignored for $|z| \ll 0.64$ km and $|y| \ll 875$ km (i.e., latitude $\ll 8°$). With these conditions satisfied, solu-

tions obtained to an initial value problem for sinusoidal forcing at the surface show that an upward propagation of phase would be expected associated with the propagation of a subsurface maximum in v downward. For longer time, the response to steady forcing at a frequency σ has a maximum along a line $z = \sigma y/N$ which is associated with the IKW ray path, with an upward propagation of phase in the vicinity of the ray path. Since the ray path is a function of σ, the response to a wind with a general frequency spectrum and a step function at $y = 0$ will consist of many rays emanating from $y = 0$, $z = 0$, and an upward propagation of phase will be observed near $y = 0$ over much of the depth.

We may also examine the conditions for which the effects of a surface are not felt. For impulsive forcing at a point on the surface the disturbance takes the form of a nonuniform wavetrain of free vertically propagating coastal Kelvin waves with local frequencies and wavenumbers, when the local vertical wavelength is much less than the distance to the surface. Typical parameters for the Peru coast ($N = 4 \times 10^{-3}$ s^{-1}, $\lambda_y = 1000$ km) give a vertical wavelength $\lambda_z \approx 0.7$ km and $c_z = 30$ m day^{-1} for $T = 25$ days. This estimate for λ_z indicates that it is unlikely that the low frequency signal in Fig. 1, which is measured at depths $|z| < 0.8$ km, i.e., $|z| \leqslant \lambda_z$, may be explained in terms of a free wave with a single frequency or wavenumber.

For forcing by a traveling wind, a standing component that decays with depth from the surface and that is trapped within a Rossby radius of the coast is forced for $\sigma/l < 0$ (poleward traveling wind) and $\sigma/l > 0$ (equatorward traveling wind). For $\sigma/l < 0$, an additional propagating component is forced, which represents a coastally trapped IKW with negative vertical group velocity and upward phase propagation. The response to forcing by a wind stress that is standing in the alongshore direction may be obtained by summing the effects of traveling waves with $\sigma/l > 0$ and $\sigma/l < 0$. For this case, downward propagating waves will be generated by the poleward propagating component of the wind while a surface trapped response will be generated by both poleward and equatorward traveling components of the wind. For $|z| > |\sigma/Nl|$, the surface trapped component is small compared to the vertically propagating component. With the parameters chosen above, the vertically propagating IKW is the dominant response for $z \leqslant -115$ m, i.e., below 115 m one would expect to see an upward propagation of phase associated with downward propagating IKWs, while above 115 m the surface trapped component of the forced response will be important and a more complicated phase dependence with depth would be expected.

The observations shown in Fig. 1 are in qualitative agreement with predictions for forcing near the equator by a traveling wind of large spatial extent. At 5°S latitude, with $|y| \approx 550$ km (the approximate distance from the equator to the ESACAN array), $T \approx 25$ days and $N \approx 4 \times 10^{-3}$ s^{-1}, the subsurface maximum propagates downward at about 40 m day^{-1} and intersects the IKW ray path at about 400 m depth. Additional measurements for longer times are needed, however, to obtain a more accurate description of low frequency phenomena along the Peru coast at low latitudes.

Finally, we point out several interesting questions: 1) do low frequency waves that are forced along the equator and that propagate vertically turn at the intersection of the equator with the South American coast and travel north and south as vertically propagating IKWs? 2) can vertically propagating IKWs transfer momentum downward and generate a mean flow? These questions suggest avenues for further theoretical studies.

Acknowledgments. This research was supported by the Oceanography Section of the National Science Foundation for R.D.R. under Grants OCE-7803382 and OCE-8024116 and for J.S.A. under Grants OCE-7826820 and OCE-8017929. The authors thank Dr. K. H. Brink for helpful discussions.

APPENDIX A

Solutions for Slowly Varying f

In this section we treat f as a slowly varying function of y, so that $f = f(\eta)$, $\eta = \beta y$, and $\beta \ll 1$. The equations that describe the problem and that may be derived from (2.1) with the above definition for f are (2.6), (2.8), (2.9) and

$$[p_{xx} + (f/N)^2 p_{zz}]_t + f_y p_x = 0. \tag{A1}$$

In a manner similar to the method used in Section 2, we seek a solution to (A1) in terms of the Fourier cosine transform. The transformed problem is (2.18b, c) and

$$[\hat{p}_{xx} - (fm/N)^2 \hat{p}]_t + f_y \hat{p}_x = 0. \tag{A2}$$

where the transform is defined by (2.17).

The solution to (A2) may be written

$$\hat{p} = \hat{p}_0 + \hat{p}_1, \tag{A3}$$

where $\hat{p}_1$ is assumed to be a small perturbation ($\hat{p}_1 \ll \hat{p}_0$), and where

$$\hat{p}_0 = \hat{Y}_0 \exp(-fmx/N). \tag{A4}$$

The problem for $\hat{p}_1$ is

$$[\hat{p}_{1xx} - (fm/N)^2 \hat{p}_1]_t = f_y \hat{Y}_0 (fm/N) \exp(-fmx/N). \tag{A5}$$

The solution to (A5) subject to (2.18c) is

$$\hat{p}_1 = \hat{Y}_1 \exp(-fmx/N) - \tfrac{1}{2}\hat{Y}_{1p} x \times \exp(-fmx/N), \tag{A6}$$

where

$$\hat{Y}_{1pt} = \hat{Y}_0 f_y. \tag{A7}$$

Therefore the total solution for $\hat{p}$ is (absorbing Y_1 in Y_0)

$$\hat{p} = (\hat{Y}_0 - \tfrac{1}{2}\hat{Y}_{1p}x)\exp(-fmx/N). \quad \text{(A8)}$$

We now use (A7) and (A8) in the remaining boundary condition (2.18b) to obtain

$$-(m/N)\hat{Y}_{0t} + \hat{Y}_{0y} - \tfrac{1}{2}\hat{Y}_0(f_y/f) = \tau(y, t). \quad \text{(A9)}$$

Eq. (A9) is a forced first-order wave equation which includes a slowly varying Coriolis parameter. The transformation $\hat{Y}_0 = f^{1/2}\hat{Y}'_0$ yields

$$-(m/N)\hat{Y}'_{0t} + \hat{Y}'_{0y} = f^{-1/2}(\eta)\tau(y, t). \quad \text{(A10)}$$

Eq. (A10) for the scaled variable $\hat{Y}'_0$ is similar to (2.20), the forced wave equation obtained for constant f, but with a factor of $f^{-1/2}(\eta)$ multiplying the forcing function. For $\tau = 0$, the free wave behavior is recovered, implying an $f^{1/2}$ growth in amplitude of an internal Kelvin wave as it propagates poleward and vertically. This amplification is a consequence of the conservation of wave energy flux and agrees with results obtained by Miles (1972) for external Kelvin waves and by Allen and Romea (1980).

With an initial condition given by (2.22), the solution for a general wind stress $\tau = \tilde{F}(y)\tilde{T}(t)$ is (2.25), where

$$p_D = -(2N/\pi)\int_0^\infty \{f(\beta y)/f[\beta(y + Nt/m)]\}^{1/2} \times \tilde{F}(y + Nt/m)\exp(-fmx/N)m^{-1} \times \cos mz\, dm. \quad \text{(A11)}$$

For forcing given by (3.1) (Example A) or (3.11) (Example B), the f-plane results are similar to the solutions obtained with (A11) with the rescaling: p (slowly varying f) $= f^{1/2}p$ (f-plane).

The formulation with a β-plane also provides an approximate condition for coastal trapping. Substitution of (2.11) in (A1) gives

$$\phi(x) = \exp\langle\{-\tfrac{1}{2}i(\beta/\omega) - [(fm/N)^2 - \tfrac{1}{4}(\beta/\omega)^2]^{1/2}\}x\rangle \quad \text{(A12)}$$

Substitution for m from (2.15) gives the trapping condition $(fl)^2 > \frac{1}{2}\beta^2$. This requirement is the same as the baroclinic trapping condition given in Allen and Romea (1980, Eq. (4.2)) for a two-layer ocean. For the limit $m \to 0$, the more restrictive barotropic trapping condition $(\omega l)^2 > \frac{1}{4}\beta^2$ applies.

APPENDIX B

Generalized Integral Transform in x

The solution to (2.3) is derived here in an alternate manner with a generalized integral transform in x. In this case, boundary conditions (2.6) and (2.8) are replaced by the equivalent conditions

$$p_{zt} = -(N^2/f)\tau(y, t)\delta(x), \quad \text{at} \quad z = 0, \quad \text{(B1)}$$

$$p_{xt} + fp_y = 0, \quad \text{at} \quad x = 0, \quad \text{(B2)}$$

where here the Ekman suction in the upper coastal corner is represented by a delta function at $x = O(B1)$.

We express p and τ as Fourier integrals in time and in y, i.e.,

$$[\tilde{\tau}(l, \omega), \tilde{p}(x, l, z, \omega)] = \int_{-\infty}^{\infty}\int_{-\infty}^{\infty}[\tau(y, t), p(x, y, z, t)] \times \exp(-i\omega t)\exp(-ily)dtdy, \quad \text{(B3)}$$

$$[\tau(y, t), p(x, y, z, t)] = (2\pi)^{-1}\int_{-\infty}^{\infty}\int_{-\infty}^{\infty}[\tilde{\tau}(l, \omega), \tilde{p}(x, l, z, \omega)] \times \exp(i\omega t)\exp(ily)d\omega dl. \quad \text{(B4)}$$

Utilization of (B3) in (2.3), (2.9), (B1) and (B2) gives

$$\tilde{p}_{xx} + (f/N)^2\tilde{p}_{zz} = 0, \quad \text{(B5)}$$

$$\tilde{p}, \tilde{p}_x, \tilde{p}_z < \infty, \quad \text{as} \quad x \to \infty, \quad z \to -\infty, \quad \text{(B6)}$$

$$\tilde{p}_z = iN^2(f\omega)^{-1}\tilde{\tau}\delta(x), \quad \text{at} \quad z = 0, \quad \text{(B7)}$$

$$\tilde{p}_x + f(l/\omega)\tilde{p} = 0, \quad \text{at} \quad x = 0, \quad \text{(B8)}$$

plus appropriate radiation conditions for $x \to \infty$, $z \to -\infty$.

Eq. (B8) is satisfied by the transform

$$\tilde{p}(x, l, z, \omega) = \int_0^\infty \Phi(\alpha, l, z, \omega) \times [\sin\alpha x - \omega(fl)^{-1}\alpha\cos\alpha x]d\alpha + W(z, l, \omega)H(\omega/l)\exp(-flx/\omega), \quad \text{(B9)}$$

where the last term is present only for $(l/\omega) > 0$. The inverse transform variables Φ and W are given by

$$\Phi(\alpha, l, z, \omega) = (2/\pi)[1 + (\omega\alpha)^2(fl)^{-2}]^{-1} \times \int_0^\infty \tilde{p}(\sin\alpha x - \omega\alpha(fl)^{-1}\cos\alpha x]dx, \quad \text{(B10)}$$

$$W(z, l, \omega) = 2f(l/\omega)\int_0^\infty \tilde{p}\exp(-flx/\omega)dx, \quad (\omega/l) > 0. \quad \text{(B11)}$$

We obtain the transformed problem for Φ by multiplying (B5) by $\sin\alpha x - \omega\alpha(fl)^{-1}\cos\alpha x$, integrating over x from 0 to ∞, and integrating by parts where appropriate. The result is

$$\Phi_{zz} - (N\alpha/f)^2\Phi = 0, \quad \text{(B12)}$$

$$\Phi_z < \infty, \quad \text{as} \quad z \to -\infty, \quad \text{(B13)}$$

with solution

$$\Phi = A(\alpha, l, \omega)\exp(N\alpha z/f). \quad \text{(B14)}$$

For $l/\omega > 0$, $W(z)$ is obtained by multiplying (B5) by $\exp(-flx/\omega)$ and integrating over x from 0 to ∞. This yields

$$W = W_0(l, \omega) \exp(-iNlz/|\omega|), \quad (l/\omega) > 0, \quad \text{(B15)}$$

where the negative root is chosen in (B15) to satisfy the radiation condition, giving a downward flux of wave energy. We find A and W_0 by taking the transform of (B7) and applying that as a boundary condition at $z = 0$ on (B14) and (B15). This gives

$$W_0 = -(2N/|\omega|)\tilde{\tau}, \ (\omega/l) > 0, \quad \text{(B16)}$$

$$A = -i(2/\pi)N(fl)^{-1}[1 + (\omega\alpha)^2(fl)^{-2}]^{-1}\tilde{\tau}. \quad \text{(B17)}$$

The total solution is

$$\tilde{p}(x, l, z, \omega) = \int_0^\infty A(\alpha, l, \omega)[\sin\alpha x - \omega\alpha(fl)^{-1}\cos\alpha x] \times \exp(Nz\alpha/f)d\alpha + H(\omega/l)W_0(l, \omega)\exp(-flx/\omega) \times \exp(-iNlz/|\omega|). \quad \text{(B18)}$$

With a particular forcing τ the pressure may now be calculated from (B4), (B16), (B17) and (B18) and the velocities computed using (2.1a) and (2.4a,b).

As a simple example, consider a traveling plane wave coastal wind stress where

$$\tau(y, t) = \tau_C \exp(-i\sigma t + il_0 y). \quad \text{(B19)}$$

The solution for p is

$$p = 2N\tau_C \exp[-i(\sigma t - l_0 y)]\{-i(\pi f l_0)^{-1} \times \int_0^\infty [\sin\alpha x + \sigma\alpha(fl_0)^{-1}\cos\alpha x] \times [1 + (\sigma\alpha)^2(fl_0)^{-2}]^{-1}\exp(N\alpha z/f)d\alpha - H(-\sigma/l_0)|\sigma|^{-1}\exp(fl_0 x/\sigma) \times \exp(-iNl_0 z/|\sigma|)\}. \quad \text{(B20)}$$

Evaluation of the integral in (B20) yields (3.23), where l in (3.23) is equal to l_0 in (B20).

REFERENCES

Allen, J. S., 1973: Upwelling and coastal jets in a continuously stratified ocean. *J. Phys. Oceanogr.*, **3**, 245–257.

——, and R. D. Romea, 1980: On coastal waves trapped at low latitudes. *J. Fluid Mech.*, **98**, 555–585.

Brink, K. H., J. S. Allen and R. L. Smith, 1978: A study of low-frequency fluctuations near the Peru coast. *J. Phys. Oceanogr.*, **8**, 1025–1041.

Gradshteyn, I. S., and I. M. Ryzhik, 1980: *Tables of Integrals, Series, and Products,* Academic Press, 1160 pp.

Huppert, H. E., and M. E. Stern, 1974: Ageostrophic effects in rotating stratified flows. *J. Fluid Mech.*, **62**, 369–385.

McCreary, J. P., 1981: A linear stratified ocean model of the coastal undercurrent. *Phil. Trans. Roy. Soc. London,* **A298**, 603–635.

Miles, J. W., 1972: Kelvin waves on oceanic boundaries. *J. Fluid Mech.*, **55**, 113–127.

Pedlosky, J., 1969: Linear theory of the circulation of a stratified ocean. *J. Fluid Mech.*, **35**, 185–205.

——, 1974: On coastal jets and upwelling in bounded basins. *J. Phys. Oceanogr.*, **4**, 3–18.

Philander, S. G. H., 1978: Forced oceanic waves. *Rev. Geophys. Space Phys.*, **16**, 15–46.

Picaut, J., 1981: Seasonal coastal upwelling in the eastern Atlantic. *Trop. Ocean-Atmos. Newsletter,* **5**, 2–3 (Unpublished manuscript).

Romea, R. D., and R. L. Smith. 1983: Further evidence for coastal trapped waves along the Peru coast. *J. Phys. Oceanogr.*, **13**, 1341–1356.

Smith, R. L., 1978: Poleward propagating perturbations in sea level and currents along the Peru coast. *J. Geophys. Res.*, **83**, 6083–6092.

Weisberg, R. H., A. Horigan and C. Colin, 1978: Equatorially trapped Rossby-gravity wave propagation in the Gulf of Guinea. *J. Mar. Res.*, **37**, 66–86.

Whitham, G. B., 1974: *Linear and Nonlinear Waves,* Wiley and Sons, 636 pp.

Wunsch, C., 1977: Response of an equatorial ocean to a periodic monsoon. *J. Phys. Oceanogr.*, **7**, 497–511.

——, 1978: Observations of equatorially trapped waves in the ocean: A review prepared for equatorial workshop, July 1977. *Review papers of Equatorial Oceanography,* FINE (FGGE/INDEX/NORPAX Equatorial) Workshop Proceedings.